2025 IEEE/SICE International Symposium on System Integration (SII)
January 21-24, 2025, Munich, Germany

Inducibility Analysis of Pedestrian's Interactive Behavior

Kentaro Sugiura[1], Hiroyuki Okuda[1], Mizuho Aoki[1], Kazuma Uchida[1], Tatsuya Suzuki[1]

***Abstract*— As the application fields of Autonomous Mobile Robots (AMRs) expand, stress-free interaction with people around them becomes more important. AMRs are highly required to interact with pedestrians like human-human interaction. This paper proposes a new measure, 'Inducibility,' expressing how AMR's behavior can induce (control) the other pedestrian's behavior. In particular, this paper discusses two kinds of inducibility measures: one is based on the sensitivity of decision-making, and the other one is based on the controllability gramian for the state space model of the interactive behavior. Finally, the validity of these two measures is evaluated based on data on interaction behaviors, and typical applications of these measures are discussed.**

I. INTRODUCTION

The demand for Autonomous Mobile Robots (AMRs) is growing due to innovations in robotics technology and a shortage of labor [1]. Consequently, AMRs are increasingly being used in environments where they coexist with pedestrians. For example, delivery robots operating in urban areas [1], transport robots in factories [2], personal mobility devices such as electric wheelchairs [3], and so on. AMRs are highly required to interact with pedestrians like human-human interaction.

In the natural interactive behavior, pedestrians appropriately switch the two strategies, 'active strategy' and 'passive strategy.' The active strategy is to prioritize own actions and goals and try to induce the other pedestrian's behavior. The passive strategy is to prioritize the other person's actions and goals and adjust their actions accordingly [4]. For example, Figure 1 assumes a situation where Ped.A wants to turn left at the intersection on the path. In Fig. 1a, Ped.A chooses the active strategy and induces Ped.B's behaviors, resulting in smooth interaction. In contrast, Figure 1b shows Ped.A chooses the passive strategy and decreases his/her movement efficiency by adjusting Ped. B's behaviors.

The optimal interaction strategy depends on the scene and scenario, such as whether it is an urban area or a hospital and hurry-up or enough time. A few studies have tried to design the switching scenario for the strategies, using data-driven methods, such as reinforcement learning [5] and genetic algorithms [6]. Although these studies have shown good behavior performance, the switching scenario's explainability is obscure and not fully discussed yet.

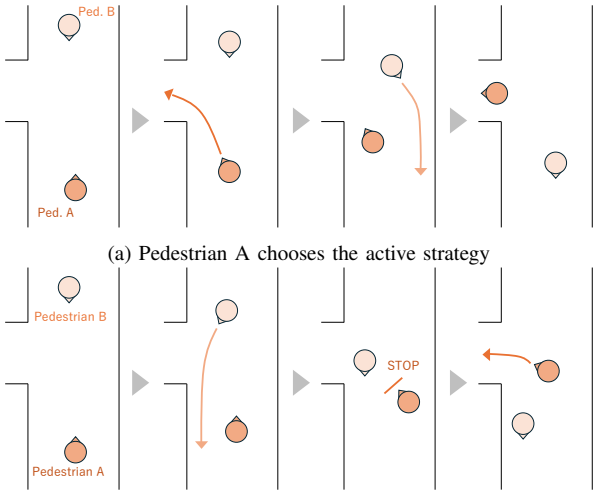

(a) Pedestrian A chooses the active strategy

(b) Pedestrian A chooses the passive strategy

Fig. 1: Example of active and passive strategies

It is highly recommended to analyze pedestrian behavior and to exploit the pedestrian behavior model to realize explainable interaction planning. Research on pedestrian behavior models can be divided into two categories: dynamical models-based approach and machine learning-based approach. The former includes models such as the Social Force Model [7], [8], which assumes forces acting on pedestrians, such as the attractive force towards their destination and the reaction force from obstacles, within a potential field framework. The latter category includes studies that model pedestrian trajectories using Neural Networks [9], [10] or represent pedestrian behavior with probabilistic measure using Bayesian inference [11].

On the other hand, previous research on pedestrian behavior analysis has focused on the analysis of the walking speed, path [12], eye direction [13], and so on. Although these quantities are useful for understanding pedestrian behavior, it is not sufficient to discuss the interaction with another pedestrian due to the lack of the explicit interaction model.

Therefore, this paper proposes a new quantity 'Inducibility,' which expresses how the pedestrian can induce (control) the other pedestrian's behavior. This paper discusses two kinds of model-based inducibility measures: one is based on the sensitivity of the decision-making model, and the other one is based on the controllability gramian for the state space model of the interactive behavior.

*This work is supported by Toyota Motor Corporation, 1 Toyota-Cho, Toyota City, Aichi Prefecture 471-8571, Japan, and partly supported by Tateisi Science and Technology Foundation.

[1]Kentaro Sugiura, Hiroyuki Okuda, Mizuho Aoki, Kazuma Uchida, and Tatsuya Suzuki are with the Department of Mechanical Systems Engineering, Graduate School of Engineering, Nagoya University, Furo-cho, Chikusa-ku, Nagoya, Aichi, Japan, sugiura.kentaro.c3@s.mail.nagoya-u.ac.jp, h_okuda@nuem.nagoya-u.ac.jp, aoki.mizuho.s0@s.mail.nagoya-u.ac.jp, uchida.kazuma.g3@s.mail.nagoya-u.ac.jp, t_suzuki@nuem.nagoya-u.ac.jp

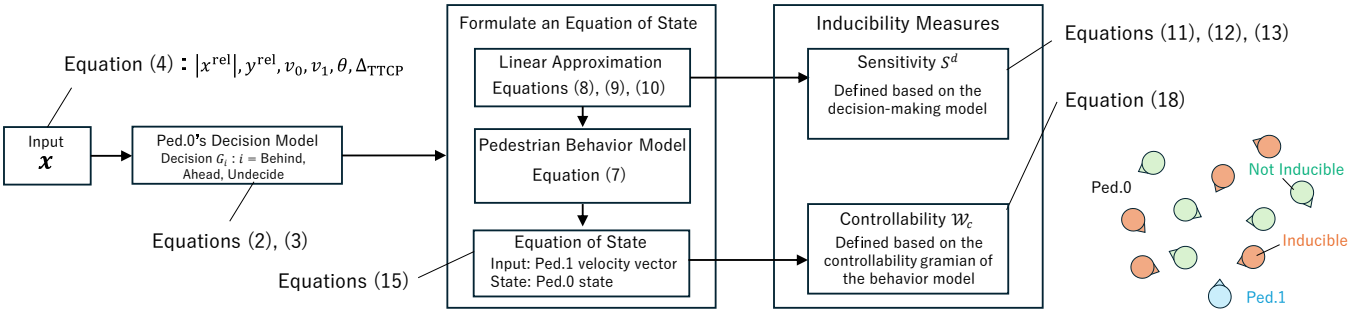

Fig. 2: Schematic of the inducibility measures
1. Sensitivity measure ; Sensitivity measure is defined based on the decision-making model
2. Controllability measure ; Controllability measure is defined based on the controllability gramian of the behavior model

Finally, the validity of the proposed two measures is evaluated based on data on interaction behavior.

The contributions of this study are summarized as follows:

- Pedestrian's reflective behavior to another pedestrian is modeled by using a logistic regression model.
- Two kinds of new 'inducibility measures' are defined based on the behavior model. One is calculated based on the sensitivity of the decision-making model and the other one is based on the controllability gramian for the state space model of the interactive behavior.
- The effectiveness of the proposed inducibility measure is verified and discussed by several experimental data of the interactive behavior.

II. Target Task and Measurement

First, pedestrians' interactions are observed in an experimental environment shown in Fig. 3a [14]. The original goal of this study is to conduct experiments involving AMRs and pedestrians. However, this paper obtained data from pedestrian-to-pedestrian interaction experiments as a preliminary step. The environment is assumed to be a semi-open space where the range for moving space is restricted by a circle.

The walking behaviors of two to five pedestrians were measured in this experiment. However, only the data from the two-pedestrian interaction scenario was used and analyzed in this paper to simplify the verification of the concept of the proposed method. When they heard a starting bell, the two pedestrians, Ped.0 and Ped.1 (Fig. 3a), started walking from some locations to the other location on the circle. During the walking, two pedestrians may interact with each other. During the experiment, the positions and postures of their heads and backs were measured by the motion capture system, Optitrack®.

All pedestrians have hand-held devices with LED monitors to check the next goal and joysticks to input their decisions. The pedestrians were asked to push or pull the joystick when they decided to go ahead of another pedestrian or to yield, respectively. Then, the pedestrian's decision, g, took one of three states, 'Ahead' (G_A), 'Behind' (G_B), or 'Undecided' (G_U), which was the state when no input was given: $g \in \{G_A, G_B, G_U\}$.

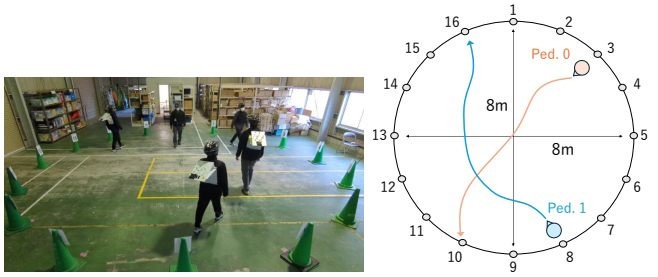

(a) Interactions measurement (b) Interaction situations

Fig. 3: Pedestrian observation experiment

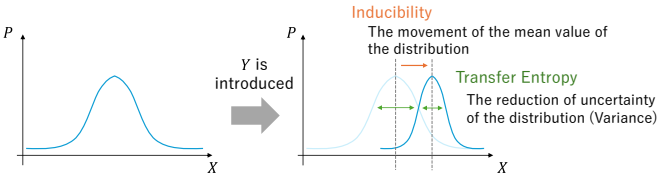

Fig. 4: Difference between 'Entropy' and 'Inducibility'

All data were recorded every 0.1 [sec]. Sixteen subjects participated in the experiment, and 3360 trials (6.5 h) were recorded in total (for 16 subjects). In adherence to ethical standards, informed consent was obtained from all the participants before the experiment.

III. Modeling of Pedestrian's Behavior

A. Overview of proposed method

This study investigated quantitative measures to evaluate how a pedestrian can induce another pedestrian.

The proposed indices were calculated using the following three steps (Fig. 2):

1) Measure the walking behaviors of pedestrians during interaction (section II).
2) Identify an interactive behavior model of pedestrians based on the measurements.
3) Compute the inducibility measure using the obtained behavior model.

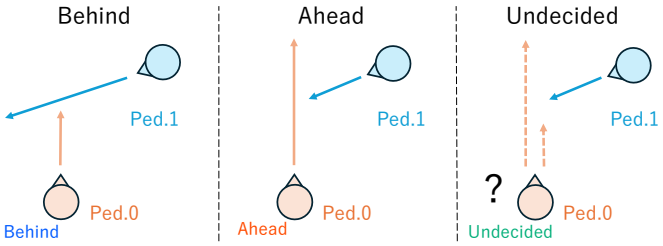

Fig. 5: Definition of pedestrian decision

There are studies on AMR behavior planning that use 'measures' similar to this research [15]. Some studies proposed a measure that quantifies the extent to which the uncertainty of other agents' behavior can be reduced, such as transfer entropy [15] or entropy of decision [16]. It is assumed that entropy represents the uncertainty in human decision-making, and when this value is low, it indicates situations where humans can make decisions more easily. Therefore, a human-friendly behavior planning is established by solving the entropy minimization problem [17], [18]. The difference between the measures proposed in this study and entropy lies in whether it involves the movement of the mean value of the human state distribution or the variance of the human state distribution (Fig. 4). This study aims to quantify 'how inducible the pedestrian is.' Therefore, this study proposes a new measure, 'Inducibility' to determine when and how the state distribution can be moved (induced).

B. Modeling of pedestrian's behavior

As the first step, an interactive behavior model of pedestrians is identified. Based on the assumption that pedestrian behavior consists of three elements, 'recognition,' 'decision,' and 'motion' the behavior was modeled as a probabilistic hybrid dynamical system[19]. To construct the model, the discrete decisions of a pedestrian, i.e., decisions are defined in a top-down manner. They are 'Behind,' 'Ahead,' and 'Undecided' (Fig. 5). The decision model is developed by using a logistic regression model (LRM) [20], [21]. Second, different motion models are assigned to the corresponding decisions, 'Behind,' 'Ahead,' and 'Undecided,' respectively.

1) Modeling decision-making of pedestrian: A logistic regression model is used to model the pedestrian's decision-making from the viewpoint of mathematical manipulability. The relative information from Ped.0 to another, Ped.1, is used as an explanatory variable ($\boldsymbol{x}(k)$), and the decision of Ped.0 is regarded as an objective variable, $g_0(k) \in \{G_B, G_A, G_U\}$, as follows:

$$g_0(k) = \begin{cases} G_B & : \text{Ped.0 goes behind Ped.1,} \\ G_A & : \text{Ped.0 goes ahead Ped.1,} \\ G_U & : \text{Ped.0 yet to decide} \end{cases} \quad (1)$$

where k represents discrete time.

Then, a logistic regression model that outputs the probabilities of three events, $E_i(k) := [g_0(k) = G_i]$, is defined as follows:

TABLE I: Definition of variables of the pedestrian model

Difference in Times to Cross Point	$\Delta_{\mathrm{TTCP}}(k)$	[s]
Relative Position of Ped.1	$x(k), y(k)$	[m]
Ped.0 Walking Speed	$v_0(k)$	[m/s]
Ped.1 Walking Speed	$v_1(k)$	[m/s]
Rel. Angle of Ped.1 pos. from Ped.0 Head Direction	$\theta(k)$	[rad]

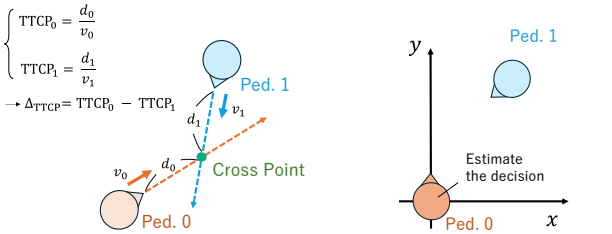

(a) Definition of Δ_{TTCP} (b) Definition of coordinates

Fig. 6: Definition for pedestrian model

$$P(E_{i\in\{B,A\}}(k)|\boldsymbol{x}(k)) = \frac{\exp(\boldsymbol{\eta}_i \boldsymbol{x}(k))}{1+\sum_{r\in\{B,A\}}\exp(\boldsymbol{\eta}_r \boldsymbol{x}(k))}, \quad (2)$$

$$P(E_U(k)|\boldsymbol{x}(k)) = \frac{1}{1+\sum_{r\in\{B,A\}}\exp(\boldsymbol{\eta}_r \boldsymbol{x}(k))} \quad (3)$$

where $\boldsymbol{x}(k)$ represents the measured explanatory variables, and $\boldsymbol{\eta}_{i\in\{B,A\}}$ are coefficients estimated from the measured data using the maximum likelihood estimation method [22]. The explanatory variable, $\boldsymbol{x}(k)$, of the model at discrete time k is defined as follows:

$$\boldsymbol{x}(k) = \left[|x^{\mathrm{rel}}(k)|,\ y^{\mathrm{rel}}(k),\ v_0(k),\ v_1(k),\ \theta(k), \Delta_{\mathrm{TTCP}}(k)\right]^\top \quad (4)$$

where each element is defined in Table I. $|x^{\mathrm{rel}}(k)|$, $y^{\mathrm{rel}}(k)$ are the relative $x(k)$ and $y(k)$ coordinate distances from Ped.0 to Ped.1, and $v_0(k)$, $v_1(k)$ are the absolute walking speeds of Ped.0 and Ped.1, respectively. $\theta(k)$ is the relative angle of Ped.1's direction measured by motion capture from the heading direction of Ped.0. $\Delta_{\mathrm{TTCP}}(k)$, is the difference in the $\mathrm{TTCP_i}(k)$ values, which are 'time to the crossing point,' calculated by the predicted walking paths of each pedestrian, $i \in \{0,1\}$, as shown in Fig. 6a,

$$\Delta_{\mathrm{TTCP}}(k) = \mathrm{TTCP}_0(k) - \mathrm{TTCP}_1(k), \quad (5)$$

$$= \frac{d_0(k)}{v_0(k)} - \frac{d_1(k)}{v_1(k)} \quad (6)$$

Note that variable $|x^{\mathrm{rel}}(k)|$ is taken as an absolute value of $x^{\mathrm{rel}}(k)$ based on the assumption that humans perform symmetric cognition and decision.

In this study, a simple logistic regression model was used as the probability decision-making model of the pedestrian's decision because the main contribution of this paper is to derive and confirm the quantified measure for the mutual influence between pedestrians.

In addition, the required computational burden or quantity of learning data could be kept small with this simple model, which will be a significant advantage when applied to AMR

behavior planning in the future. Although more complex models such as neural networks [9], [10] could realize higher accuracy of the input-output relationship, the extension to those more complex models is left for our future work.

2) Modeling motion of pedestrian: The motion model describes the pedestrian's physical behavior according to the decision in the decision model explained in the previous section.

In particular, the walking speed of the pedestrian in the relative coordinate system is regarded as the output of the motion model, as shown in Fig. 6b. Output $v_0(k+1)$, the walking speed of Ped.0, is represented by the probability-weighted average[19], i.e. expectation, of the reference speed assigned to each decision together with the discrete-time first-order delay as follows:

$$\begin{aligned} v_0(k+1) &= (1-\alpha\Delta k)v_0(k) \\ &+\alpha\Delta k \left[V_B^{\mathrm{ref}}, V_A^{\mathrm{ref}}, V_U^{\mathrm{ref}}\right] \left[P(E_B(k)), P(E_A(k)), P(E_U(k))\right]^\top \end{aligned} \quad (7)$$

Here, V_i^{ref} $(i \in \{B,A,U\})$ are the reference speed related to each decisions, $g_0(k) = G_i$. The reference speeds are set to be V_B^{ref} =0.8 m/s, V_A^{ref} =1.1 m/s, and V_U^{ref} =1.4 m/s. α, the time constant, is set to be α =2.5, and Δk is the time step of the experimental data, and set to be $\Delta k = 0.1$ [sec].

IV. Inducibility measure for interactive behavior

A. Inducibility measure 1: Sensitivity of decision

At the first measure of the inducibility, the sensitivity measure of the decision model is considered. The controllability ellipsoid of a system is often used for influence analysis (or sensitivity analysis) and the proposed index is similar to this idea. The sensitivity of the decision probability of Ped.0 is influenced by the walking speed of Ped.1.

Since the target model (decision model of Ped.0) is nonlinear, Taylor expansion around the operating point $\overline{\boldsymbol{x}}(k)$, is applied to linearize the decision model.

$$\begin{aligned} P(E_B(k)|\boldsymbol{x}(k)) &= P(E_B(k)|\overline{\boldsymbol{x}}(k)) \\ &+ \left.\frac{\partial P(E_B(k)|\boldsymbol{x}(k))}{\partial v_1(k)}\right|_{v_1(k)=\overline{v_1}} (v_1(k)-\overline{v_1}), \quad (8) \\ P(E_A(k)|\boldsymbol{x}(k)) &= P(E_A(k)|\overline{\boldsymbol{x}}(k)) \\ &+ \left.\frac{\partial P(E_A(k)|\boldsymbol{x}(k))}{\partial v_1(k)}\right|_{v_1(k)=\overline{v_1}} (v_1(k)-\overline{v_1}), \quad (9) \\ P(E_U(k)|\boldsymbol{x}(k)) &= P(E_U(k)|\overline{\boldsymbol{x}}(k)) \\ &+ \left.\frac{\partial P(E_U(k)|\boldsymbol{x}(k))}{\partial v_1(k)}\right|_{v_1(k)=\overline{v_1}} (v_1(k)-\overline{v_1}) \quad (10) \end{aligned}$$

The partial derivative coefficients are these equations defined as the Sensitivity measures, $S_{v_1}^d$, for $d \in \{B,A,U\}$:

$$S_{v_1}^B(k) = \left.\frac{\partial P(E_B(k)|\boldsymbol{x}(k))}{\partial v_1(k)}\right|_{v_1(k)=\overline{v_1}}, \quad (11)$$

$$S_{v_1}^A(k) = \left.\frac{\partial P(E_A(k)|\boldsymbol{x}(k))}{\partial v_1(k)}\right|_{v_1(k)=\overline{v_1}}, \quad (12)$$

$$S_{v_1}^U(k) = \left.\frac{\partial P(E_U(k)|\boldsymbol{x}(k))}{\partial v_1(k)}\right|_{v_1(k)=\overline{v_1}} \quad (13)$$

The sensitivity of decision-making is defined as the partial derivative coefficient to $v_1(k)$ in the decision model. Specifically, it quantifies the influence of $v_1(k)$ on the probability of each decision (a positive sensitivity value indicates an increase in probability, while a negative one indicates a decrease in probability). Note that this measure does not consider the motion model of the pedestrian, and only considers the sensitivity of the decision-making for the walking speed of another pedestrian. The sensitivity of the motion can also be computed similarly by assuming some mathematical motion model, such as the social force model or so on. Note also that this measure can be naturally extended to a case where more than two pedestrians are considered.

B. Inducibility measure 2: Controllability Gramian

In the second measure, the controllability gramian is considered. This implies how controllable Ped.0 is by the walking speed of Ped.1. By adopting the decision model (eqs. (2) and (3)), and motion model (eq. (7)), the state equation regarding the $v_1(k)$ as an input can be derived as follows:

$$\begin{aligned} \begin{bmatrix} x_0(k+1) \\ y_0(k+1) \\ v_0(k+1) \end{bmatrix} &= \begin{bmatrix} 1 & 0 & -\Delta k\cos\phi(k) \\ 0 & 1 & -\Delta k\sin\phi(k) \\ 0 & 0 & 1-\alpha\Delta k \end{bmatrix} \begin{bmatrix} x_0(k) \\ y_0(k) \\ v_0(k) \end{bmatrix} \\ &+ \alpha\Delta k \begin{bmatrix} 0 & 0 & 0 \\ 0 & 0 & 0 \\ V_B^{ref} & V_A^{ref} & V_U^{ref} \end{bmatrix} \begin{bmatrix} P(E_B(k)|\boldsymbol{x}(k)) \\ P(E_A(k)|\boldsymbol{x}(k)) \\ P(E_U(k)|\boldsymbol{x}(k)) \end{bmatrix} \end{aligned} \quad (14)$$

where state $\boldsymbol{x}(k)$ consists of the position and walking velocity of Ped.0. $\phi(k)$ is the walking direction of Ped.1 in the local frame of Ped.0.

By using Taylor expansion of decision models (eqs. (8), (9), and (10)), the state equation can be transformed as follows:

$$\begin{aligned} \begin{bmatrix} x_0(k+1) \\ y_0(k+1) \\ v_0(k+1) \end{bmatrix} &= \begin{bmatrix} 1 & 0 & -\Delta k\cos\phi(k) \\ 0 & 1 & -\Delta k\sin\phi(k) \\ 0 & 0 & 1-\alpha\Delta k \end{bmatrix} \begin{bmatrix} x_0(k) \\ y_0(k) \\ v_0(k) \end{bmatrix} \\ &+ \alpha\Delta k \begin{bmatrix} 0 & 0 & 0 \\ 0 & 0 & 0 \\ V_B^{ref} & V_A^{ref} & V_U^{ref} \end{bmatrix} \begin{bmatrix} S_{v_1}^B(k)v_1(k)+C_B(k) \\ S_{v_1}^A(k)v_1(k)+C_A(k) \\ S_{v_1}^U(k)v_1(k)+C_U(k) \end{bmatrix}, \\ \boldsymbol{x_0}(k+1) &= A(k)\boldsymbol{x_0}(k) + \begin{bmatrix} 0 \\ 0 \\ \xi_0(k)v_1(k)+\xi_1(k) \end{bmatrix}, \\ &= A(k)\boldsymbol{x_0}(k) + \begin{bmatrix} 0 & 0 \\ 0 & 0 \\ \xi_0(k) & \xi_1(k) \end{bmatrix} \begin{bmatrix} v_1(k) \\ 1 \end{bmatrix}, \\ &= A(k)\boldsymbol{x_0}(k) + B(k)\boldsymbol{u_1}(k) \end{aligned} \quad (15)$$

where $\xi_0(k)$ and $\xi_1(k)$ are the product of the output probability coefficient and reference speed, and $C_B(k)$, $C_A(k)$, and $C_U(k)$ is a constant term.

The controllability gramian for a discrete-time linear system can be expressed as follows [23]:

$$W_c^{\infty}(k) = \sum_{i=0}^{\infty} A(k)^i B(k) B(k)^{\top} (A(k)^{\top})^i \tag{16}$$

and it is known that the magnitude of the eigenvalues of $W_c^{\infty}(k)$ corresponds to the size of the reachable set over an infinite future.

Since this study used a local linear approximation at time k to obtain the linear system, it would be unnatural to consider controllability over infinite steps. Then, the controllability gramian over the finite time horizon is considered as follows [24], [25]:

$$W_c^{L}(k) = \sum_{i=0}^{L-1} A(k)^i B(k) B(k)^{\top} (A(k)^{\top})^i \tag{17}$$

Here, L is the number of steps needed to evaluate the controllability. Regarding the physical meaning of the controllability gramian, this measure is expected to evaluate the effect of input changes on the state changes, i.e., the effect of changes in the speed of Ped.1 on the changes in the position and speed of Ped.0. Because time interval Δk was 0.1 [sec] in our measurement, $L = 10$ was used to consider time duration $L\Delta k = 1.0$ [sec] for controllability evaluation.

Finally, a scalar measure from the controllability gramian $W_c^L(k)$ is derived as a measure of the inducibility of Ped.0 by Ped.1. Since $W_c^L(k)$ is a matrix, the magnitude of $W_c^L(k)$ is computed using the trace [26] or determinant, and defined as a scalar inducibility measure, $\mathcal{W}_c^{Ped.0/Ped.1}(k)$:

$$\mathcal{W}_c^{Ped.0/Ped.1}(k) = \mathrm{tr}\left(W_c^L(k)\right) \tag{18}$$

V. Verification of Measure and Discussion

In this section, first, the modeling results for a pedestrian's decision are shown and discussed. Then, the validity of the proposed measures, 'Sensitivity' and 'Controllability', introduced in section II, are verified and discussed.

A. Modeling results

Because the following analysis was based on the proposed measures, which relied on the pedestrian's model, the model accuracy was first verified.

Figures 7a and 7b show the distributions of the measured and estimated intentions of Ped.0. In these figures, Ped.1 is located at the origin, and he/she walks in the y direction. In both figures, each point shows the decision, (Behind(blue), Ahead(red), or Undecided(green)) of Ped.0 at the corresponding point measured by the handheld switch or estimated by the logistic regression model.

A comparison of the measurement and modeling results is shown in Figs. 7a and 7b confirmed that the decision model could almost capture the tendency satisfactorily. The accuracy of the model in estimating the decisions was 82.6%

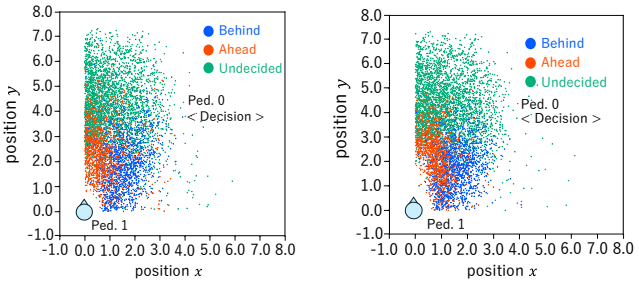

(a) Observed decision-making (b) Estimated decision-making

Fig. 7: Comparison of observed and estimated decision

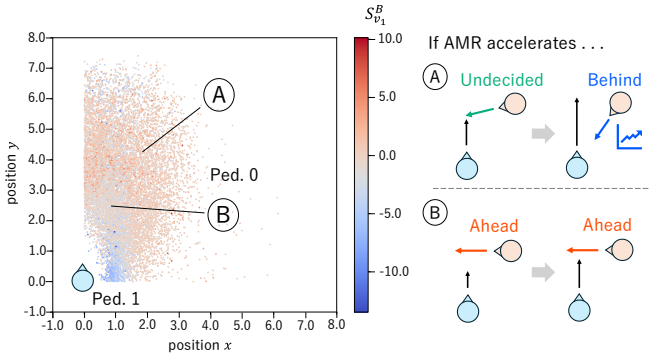

(a) Sensitivity measure of 'Behind' decision of Ped.0, S_{v1}^B

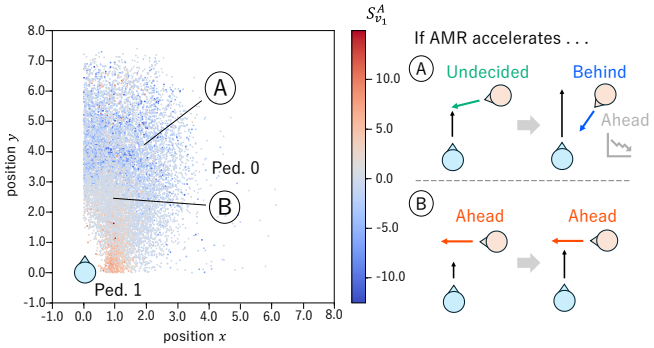

(b) Sensitivity measure of 'Ahead' decision of Ped.0, S_{v1}^A

Fig. 8: Sensitivity distribution

on average. An overlap between 'Behind' and 'Ahead' can be seen in the estimations in the bottom area, around $(x, y) = (1.0,\ 0.5)$. The modeling error in this area leads to the reliability of the measure, as described in the later analysis.

B. Analysis of inducibility using sensitivity measure

Figures 8a and 8b show the distribution of sensitivity measure $S_{v_1}^i\ (i \in B, A)$. Ped.1, who is an affecter, walked in the y direction located at the origin. A larger $\|S_{v_1}^i\|$ value in red shows the larger positive influence (with a negative influence shown in blue) on the decision probability, $P(E_i(k))$, of Ped.0 at the corresponding point, from changes in the walking speed of Ped.1 at the origin.

In Fig. 8a, the probability that Ped.0 decides to walk 'Behind' increases when Ped.1 at the origin accelerates in the case that there exists a certain distance between Ped.0 and

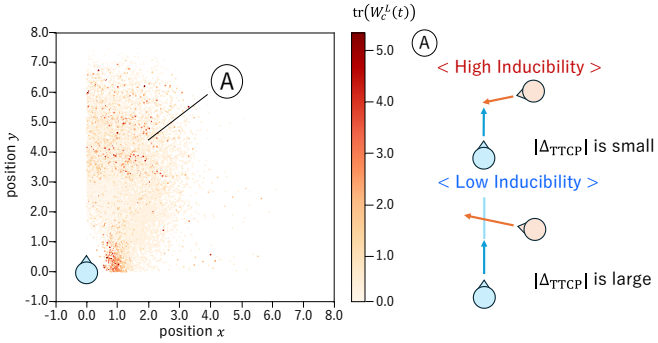

Fig. 9: Controllability distribution

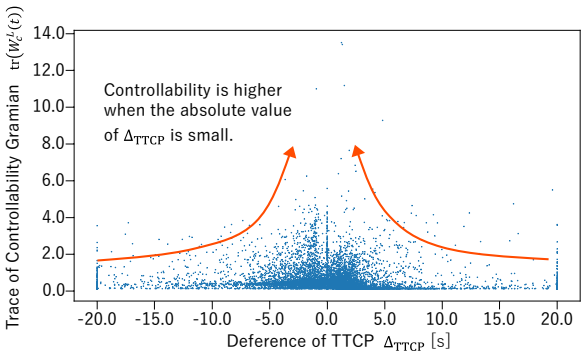

Fig. 10: Controllability measure - Δ_{TTCP} plot

Ped.1 (region A). This is because Δ_{TTCP} will be increased by an increase of the walking speed of Ped.1, which encourages Ped.0 to choose 'Behind' instead of 'Ahead' or 'Undecided.' On the other hand, in the middle part of the figure (region B: around (x,y)=(1.0, 2.0)), lower sensitivity values (light color) are distributed. This implies that it is difficult for Ped.1 to induce a decision by Ped.0 in this area as desired.

Similarly, in Fig. 8b, the probability that Ped.0 decides to walk 'Ahead' can decrease when Ped.1 to the origin accelerates in the case that there exists a certain distance between Ped.0 and Ped.1 (region A). In the middle part in Fig. 8b (region B), low sensitivity values are distributed. Thus, the inducibility, i.e., how much Ped.1 can change the decision of Ped.0 to 'Ahead' or 'Behind,' is visualized using the sensitivity measure.

Note that in the bottom area in these figures (around (x,y)=(1.0, 0.5)), the opposite sensitivity distribution is observed. This might be happened because of low accuracy in the modeling in the corresponding area. As shown in Fig. 7b, the estimated 'Behind' and 'Ahead' points are highly overlapping in this area. This implies that the sensitivity of this area has less reliability. Improving the model accuracy in this area is one of our future works.

C. Analysis of inducibility using controllability measure

Figure 9 shows the magnitude of $\mathcal{W}_c^{Ped.0/Ped.1}$ when Ped.1 walks in the y direction from the origin. The dark points in the figure show larger controllability. In the case that the Ped.0 is located at the corresponding point. As seen, two areas, the upper area around $y = 3.0$ to 7.0 (region A) and the bottom area around $(x,y) = (1.0,\ 0.5)$, show larger controllability, while the middle area between them show lower controllability. The large controllability implies that Ped.1 can control the behavior of Ped.0 (i.e., state $\boldsymbol{x_0}(k)$) with less effort. In the bottom area, although the measure shows a larger value, this result is not reliable for the same reason discussed in the analysis using the sensitivity measure. Focusing on more detail in region A, it can be found that both higher and lower controllability measure exist. This is because the position space is not suitable to discuss the controllability distribution. It was found that the controllability has strong dependency on the Δ_{TTCP}.

In Fig. 10, the relation between Δ_{TTCP} and $\mathcal{W}_c^{Ped.0/Ped.1}$ is depicted. In this figure, it can be seen that the controllability measure becomes larger according to the absolute value of Δ_{TTCP} getting close to zero. This seems to be natural considering the physical meaning of the Δ_{TTCP} and controllability.

D. Comparison between sensitivity measure and controllability measure

Finally, the two proposed measures, the sensitivity and controllability measures, are compared with each other. In general, a comparison of Figs. 8a to 9 indicates that an area with a larger sensitivity region in Figs. 8a and 8b also shows a larger controllability in Fig. 9. In this sense, the controllability measure can be considered to be similar to the sensitivity measure other than the direction in which each decision is to be induced. Another difference between them is described as follows: Although the sensitivity measure can capture the influence only on the static decision-making of another pedestrian, the controllability measure can reflect the influence on the dynamic predicted behavior of another pedestrian. This could be a significant advantage for the design of AMR strategy utilizing future prediction such as model predictive control, a dynamic time window approach, or dynamic programming.

E. Extension to the evaluation for eHMI

The applications of the inducibility measures include not only the behavioral planning of AMRs whether taking active or passive strategy but also the evaluation of the effect of the external human-machine interface (eHMI) [18], [27] designed to induce the pedestrian behavioral changes.

The effect evaluation of the eHMI on the pedestrian behavioral changes is conducted as follows: First, the output information of the eHMI is included in the explanatory variables of the pedestrian decision-making model shown in eq. (4). This enables to model of the reflective decision-making of the pedestrian for the output of the eHMI. Next, equations (2) and (3) are reformulated using Taylor expansion for the eHMI's output information as derived in eqs. (8), (9), and (10). Then, the sensitivity measure for eHMI is defined like eqs. (11), (12), and (13). Similarly, another inducibility measure, the controllability measure, is defined by including the eHMI's output information into the input $\boldsymbol{u_1}$ in eq. (15).

The extension explained in this section is available for the analysis of the effect of any type of interaction support tool.

VI. CONCLUSION

This paper has a new measure called the 'Inducibility measure.' This proposed measure can represent how another pedestrian can be induced (controlled) by a pedestrian's behavior. In particular, this paper discussed two types of inducibility measures: one is based on the sensitivity of decision-making and the other is based on the controllability gramian for the state space model of the interactive behavior.

The analysis of the interaction based on the proposed measures clarified the situations where pedestrian has been strong interactions with other pedestrian. In addition, a strong relationship between inducibility and Δ_{TTCP} has been found. In particular, it has been found that a small Δ_{TTCP} is more likely to induce the other pedestrian's behavior into some specific behavior.

Improving the modeling accuracy by changing the model structure and explanatory variables, and the application to design of the AMR planner will be our future work.

REFERENCES

[1] B. Nils, F. Stefan, and S. Stefan, "Last-mile Delivery Concepts: a Survey from an Operational Research Perspective," in *Spectrum*, vol. 43, no. 1. Springer, 2021, pp. 1–58.

[2] A. Singhal, P. Pallav, N. Kejriwal, S. Choudhury, S. Kumar, and R. Sinha, "Managing a Fleet of Autonomous Mobile Robots (AMR) Using Cloud Robotics Platform," in *Euro Conf. on Mobile Robots*. IEEE, 2017, pp. 1–6.

[3] R. Hye-Yeon, K. Je-Seong, L. Jeong-Hak, K. Hyeon, B. Su-Jin, and K. Jong-Wook, "Development of an Autonomous Driving Smart Wheelchair for the Physically Weak," in *Applied Sciences*, vol. 12, no. 1. MDPI, 2021, p. 377.

[4] K. Miyamoto, N. Watanabe, O. Nakamura, and Y. Takefuji, "Analysis of a Human Meta-Strategy for Agents with Active and Passive Strategies," in *Applied Sciences*, vol. 12, no. 17. MDPI, 2022, p. 8720.

[5] K. Miyamoto, N. Watanabe, and Y. Takefuji, "Adaptation to Other Agent's Behavior Using Meta-Strategy Learning by Collision Avoidance Simulation," in *Applied Sciences*, vol. 11, no. 4. MDPI, 2021, p. 1786.

[6] B. D. Eldridge and A. A. Maciejewski, "Using Genetic Algorithms to Optimize Social Robot Behavior for Improved Pedestrian Flow," in *Intl. Conf. on Sys., Man and Cybernetics*, vol. 1. IEEE, 2005, pp. 524–529.

[7] D. Helbing and P. Molnar, "Social Force Model for Pedestrian Dynamics," in *Physical Review E*, vol. 51, no. 5. APS, 1995, p. 4282.

[8] W. Wu, M. Chen, J. Li, B.Liu, and X. Zheng, "An Extended Social Force Model via Pedestrian Heterogeneity Affecting the Self-Driven Force," in *Transactions on Intelligent Transportation Sys.*, vol. 23, no. 7. IEEE, 2021, pp. 7974–7986.

[9] B. F. de Brito, H. Zhu, W. Pan, and J. Alonso-Mora, "Social-VRNN: One-Shot Multi-Modal Trajectory Prediction for Interacting Pedestrians," in *Conf. on Robot Learning*. PMLR, 2021, pp. 862–872.

[10] E. Stuart, L. Kunming, S. Mao, W. Stewart, S. Salah, and M. N. Eduardo, "Probabilistic Crowd GAN: Multimodal Pedestrian Trajectory Prediction Using a Graph Vehicle-Pedestrian Attention Network," in *Robotics and Automation Letters*. IEEE, 2020, pp. 5026–5033.

[11] S. Bansal, A. Bajcsy, E. Ratner, A. Dragan, and C. Tomlin, "A Hamilton-Jacobi Reachability-Based Framework for Predicting and Analyzing Human Motion for Safe Planning," in *Intl. Conf. on Robotics and Automation*. IEEE, 2020, pp. 7149–7155.

[12] R. Karim, S. Weiguo, A. R. Rasa, M. A. Khan, and N. D. Bilintoh, "Comparative Study of Multidirectional Pedestrian Flows: Insights and Dynamics," in *Physica A: Statistical Mechanics and its Applications*. Elsevier, 2024, p. 130053.

[13] L. Lévêque, M. Ranchet, J. Deniel, J.-C. Bornard, and T. Bellet, "Where Do Pedestrians Look When Crossing? A State of the Art of the Eye-Tracking Studies," in *IEEE Access*, vol. 8. IEEE, 2020, pp. 164 833–164 843.

[14] K. Uchida, N. Kodama, H. Okuda, K. Kuroda, and T. Suzuki, "Observation and Modeling of Decision-Making of Pedestrian with Interactions at X-Crossing"," in *Annual Conf. of the Society of Inst. and Ctrl Engineers*. IEEE, 2023, pp. 850–855.

[15] H. Jiang, E. A. Croft, and M. G. Burke, "Social Cue Detection and Analysis Using Transfer Entropy," in *Intl. Conf. on Human-Robot Interaction*. IEEE, 2024, pp. 323–332.

[16] H. Okuda, T. Suzuki, K. Harada, S. Saigo, and S. Inoue, "Quantitative Driver Acceptance Modeling for Merging Car at Highway Junction and its Application to the Design of Merging Behavior Control," in *Transactions on Intelligent Transportation Sys.*, vol. 22, no. 1. IEEE, 2019, pp. 329–340.

[17] A. Muraleedharan, H. Okuda, and T. Suzuki, "Pedestrian-Aware Model Predictive Controller for Design of Considerate Autonomous Driving," in *Transactions of the Society of Inst. and Ctrl Engineers*, vol. 59, no. 11. IEEE, 2023, pp. 472–483.

[18] K. Suzuki, T. Yamaguchi, H. Okuda, and T. Suzuki, "Indication of Interaction Plans Based on Model Predictive Interaction Control: Cooperation Between AMRs and Pedestrians Using eHMI," in *Annual Conf. of the Society of Inst. and Ctrl Engineers*. IEEE, 2022, pp. 1232–1237.

[19] H. Okuda, N. Ikami, T. Suzuki, Y. Tazaki, and K. Takeda, "Modeling and Analysis of Driving Behavior Based on a Probability-Weighted ARX Model," in *Transactions on Intelligent Transportation Sys.*, vol. 14, no. 1. IEEE, 2012, pp. 98–112.

[20] T. Watanabe, T. Yamaguchi, H. Okuda, T. Suzuki, R. Wakisaka, and K. Ban, "Analysis and Modeling of Traffic Participants Considering Interactions at Intersections without Traffic Signals," in *Intl. Symposium on Sys. Integration*. IEEE, 2023, pp. 1–8.

[21] J. Zhao, J. O. Malenje, Y. Tang, and Y. Han, "Gap Acceptance Probability Model for Pedestrians at Unsignalized Mid-Block Crosswalks Based on Logistic Regression," in *Accident Analysis & Prevention.*, vol. 129. Elsevier, 2019, pp. 76–83.

[22] C.-Y. J. Peng, K. L. Lee, and G. M. Ingersoll, "An Introduction to Logistic Regression Analysis and Reporting," in *The Journal of Educ Research*, vol. 96, no. 1. Taylor & Francis, 2002, pp. 3–14.

[23] S. Zhao and F. Pasqualetti, "Discrete-Time Dynamical Networks with Diagonal Controllability Gramian," in *IFAC-PapersOnLine*, vol. 50, no. 1. Elsevier, 2017, pp. 8297–8302.

[24] S. Roy and M. Xue, "Controllability-Gramian Submatrices for a Network Consensus Model," in *Sys. & Ctrl Letters*, vol. 136. Elsevier, 2020, p. 104575.

[25] K. Sugiura, M. Aoki, K. Kuroda, H. Okuda, and T. Suzuki, "Evaluation of Controllability of Interaction Between Pedestrian and Autonomous Mobile Robot in Shared Mobility Space," in *ICINCO*, vol. 2. Sitepress, 2023, pp. 249–257.

[26] M. Imran and A. Ghafoor, "Model Reduction of Descriptor Systems Using Frequency Limited Gramians," in *Journal of the Franklin Institute*, vol. 352, no. 1. Elsevier, 2015, pp. 33–51.

[27] D. Dey, A. Matviienko, M. Berger, B. Pfleging, M. Martens, and J. Terken, "Communicating the Intention of an Automated Vehicle to Pedestrians: The Contributions of eHMI and Vehicle Behavior," in *Information Technology*, vol. 63, no. 2. De Gruyter Oldenbourg, 2021, pp. 123–141.